Scientific Research Publishing

Optics and Photonics Journal, 2022, 12, 156-169
https://www.scirp.org/journal/opj
ISSN Online: 2160-889X
ISSN Print: 2160-8881

Perimeter Security System Based on Ultra-Weak Fiber Bragg Grating Array

Zhihui Luo[1,2], Hao Xiang[1,2], Yu Zhang[1,2], Bing Xu[1,2*]

[1]Hubei Engineering Research Center of Weak Magnetic-field Detection, China Three Gorges University, Yichang, China
[2]College of Science, China Three Gorges University, Yichang, China
Email: *xbwhut2018@163.com

How to cite this paper: Luo, Z.H., Xiang, H., Zhang, Y. and Xu, B. (2022) Perimeter Security System Based on Ultra-Weak Fiber Bragg Grating Array. *Optics and Photonics Journal*, **12**, 156-169.
https://doi.org/10.4236/opj.2022.126012

Received: June 11, 2022
Accepted: June 27, 2022
Published: June 30, 2022

Abstract

A perimeter security system based on ultra-weak fiber Bragg grating high-speed wavelength demodulation was proposed. The demodulation system for signal acquisition and high-speed wavelength calculation was designed based on field programmable gate array (FPGA) platform. The principle of ultra-weak fiber Bragg grating high-speed demodulation and signal recognition method were analyzed theoretically, and the Support Vector Machine model was introduced to optimize the event recognition accuracy of the system. A perimeter security experimental system containing 1000 ultra-weak fiber Bragg gratings, ultra-weak fiber Bragg grating sense optical cables with a diameter of 2.0 mm and a reflectivity of 0.01%, steel space frames and demodulation equipments was built to recognize four typical events such as knocking, shaking, wind blowing and rainfall. The experimental resulted show that the system has a spatial resolution of 1m and an acquisition frequency of 200 Hz. The joint time-frequency domain detection method is used to achieve 99.2% alarm accuracy, and 98% recognition accuracy of two intrusion events, which has good anti-interference performance.

Keywords

Perimeter Security, Ultra-Weak Fiber Bragg Grating, Vibration Sensor, Pattern Recognition

1. Introduction

Perimeter security systems can reduce or avoid personal safety risks and property damage in vital applications such as oil pipelines, storage facilities, airports, and military bases by sending fast alerts of unlawful entrance or vandalism. Passive, long-distance, low-false-positive-rate security technologies are always in

high demand in the sensor industry.

Fiber sensing technology is corrosion-resistant, electromagnetic interference-resistant and sensitive compared to traditional security technologies such as infrared detectors, video surveillance, laser beam detectors, and electronic guardrail. The perimeter security system has many advantages, such as long-distance monitoring, and has been used in many important places such as high-speed rail lines and subway tunnels [1] [2] [3] [4] [5]. Fiber perimeter security technologies include distributed sensing technologies (e.g., phase-sensitive optical time-domain reflectometer (ϕ-OTDR), Mach-Zehnder interferometer (M-ZI)), and fiber Bragg grating (FBG) semi-distributed sensing technologies [6] [7] [8] [9]. Herein, ϕ-OTDR ruses back facing Rayleigh scattered light interference to detect fiber vibration signal and is the leading distributed fiber perimeter security technique currently available. In 2020, Su *et al.* established a ϕ-OTDR-based fiber vibration sensing system [10] to monitor the rupture of substation perimeter. This system had an accuracy of 20 m but was limited by a poor signal-to-noise ratio (SNR). Because ϕ-OTDR can only monitor the invasion events qualitatively. To improve the accuracy of event identification, based on ϕ-OTDR improved distributed fiber acoustic sensor (DAS) has been proposed [11] [12]. However, it still cannot overcome the influence of Rayleigh scattering random noise. Ultra-weak fiber Bragg grating (uwFBG) has extremely low reflectivity (<0.1%), tens of thousands of sensors are allowed to be written on one fiber, and its directional reflection can effectively suppress the influence of Rayleigh scattering. In 2018, Wuhan Fengli Photoelectric Technology Co., LTD developed a new generation of weak fiber Bragg grating DAS system using a weak fiber Bragg grating array as a sensing unit. Although the SNR significantly increased to 80 dB, the false alarm rate improved modestly. The researcher (2020, Tao Xin *et al.*) designed a weak fiber Bragg grating DAS perimeter security system with low sensitivity [13]. The vibration signal of 10 - 90 Hz is effectively detected on a 2.4 km sensing optical cable, and the false alarm rate is reduced to 10%. Fiber Bragg grating, semi-distributed technology, monitors temperature and strain changes in the external environment. The signal is stable, and the false alarm rate is low and robust against environmental interference. In 2020, Wang *et al.* designed a vibration monitoring system for FBG perimeter security [14]. Experiments prove that this system can reliably monitor walking personnel within the scope of 70 m and 200 m within the range of the vehicle. However, this system only has 16 fiber Bragg grating sensors and fiber Bragg grating with large spacing and poor positioning accuracy. uwFBG's extensive capacity reuse features allow for high-density field deployment. In 2021, Chen et al. reported strain monitoring of the Hangzhou Xiasha bridge using 4118 uwFBG [15], but this system can only be applied to static, slow signal monitoring. It is difficult to collect and analyze the dynamic signal on the perimeter.

To address the complex dynamic signal collection problem and false positives in perimeter security, we propose a uwFBG-based perimeter security system.

Based on analyzing the principles of uwFBG array perimeter security, starting with hardware design and algorithms, obtain the frequency and amplitude of the vibration signal on the guardrail through high-speed demodulation. Then introduce a pattern recognition algorithm to study typical events such as percussion, shaking, wind blowing, and precipitation, and discuss the method to reduce the system false alarm rate. Finally, an experimental design of uwFBG perimeter security was established to verify the feasibility of the system scheme.

2. Principles of uwFBG-Based Perimeter Security

2.1. uwFBG-Based Perimeter Security System

Figure 1 shows the structure of the perimeter security system based on uwFBG array. It comprises a uwFBG high-speed demodulation system and uwFBG sensing optical cable. The tunable sweeping laser (TSL) in the high-speed demodulation system emits continuous wave from a wavelength range that can be set. The continuous wave is modulated into optical pulse by a semiconductor optical amplifier (SOA) and then the optical pulse is amplified with an Erbium-doped fiber amplifier (EDFA) into an optical circulator. Finally, the optical pulse enters the uwFBG array through the optical circulator. The optical signal reflected by the uwFBG array is output from the three ports of the circulator, converted into an analogue electrical signal by the photodetector, and converted into a data matrix through an analogue to digital converter (AD). System control, signal processing, and communication are completed by a FPGA board, and the model is ZYNQ7035 embedded platform. ZYNQ7035 receives PC or remote configuration instructions generates a timing signal to control TSL, AD, and SOA, and determines its spatial location according to the optical time-domain reflection signal of each uwFBG. The peak wavelength changes are obtained after gaussian fitting of the reflected signal of uwFBG. The central wavelength of each uwFBG can be demodulated out. The sensing optical cable uses elastic materials to coat the uwFBG array for the second time, and uses a buckle structure to lock it with the guardrail, so as to effectively sense the vibration of the guardrail

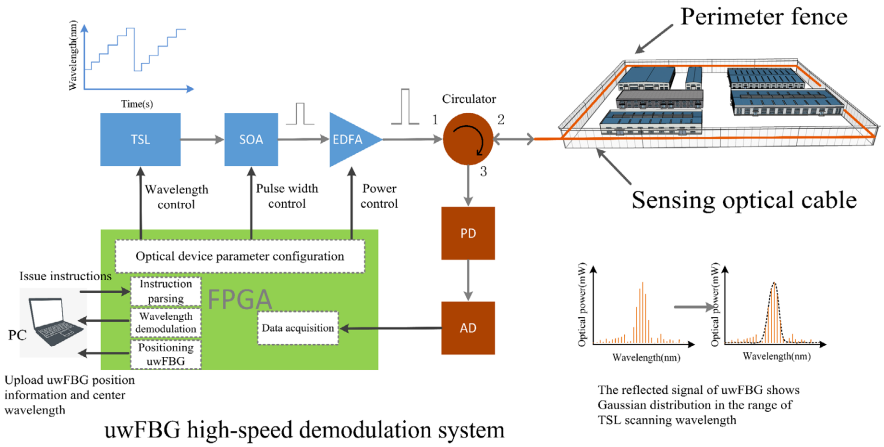

Figure 1. uwFBG-based perimeter security system.

caused by human intrusion or external impact. Additionally, the high-speed demodulation system also integrates signal analysis and alarming. FPGA transmits the central wavelength and position information of each uwFBG to the PC, and the PC shards and pre-processes the vibration signal on the cable to extract signal features. Various algorithms judge typical events, and corresponding alarm information is given.

2.2. Design of High-Speed Wavelength Demodulation Scheme

The vibration signal generated on the rigid perimeter guardrail by events such as human invasion or external impact is about 10 Hz, which requires high-speed demodulation of the wavelength changes of all uwFBG on the optical fiber, so as to obtain the vibration frequency and amplitude signals at the event point. But based on OTDR multiple pulses in the optical path of the limitation of crosstalk, the wavelength transform of TSL must wait for the optical pulse to return ultimately in last time. Assuming that the length of the fiber is L, the round-trip transmission time of an optical pulse in the whole fiber is t

$$t = \frac{2nL}{c} \tag{2.1}$$

where n is the refractive index of the core and c is the speed of light. Set scanning laser wavelength scanning width as m, scanning step for p, then, the time T required by demodulation system to complete data acquisition of uwFBG on all array is:

$$T = \frac{2nmL}{pc} \tag{2.2}$$

The maximum scanning frequency f of the uwFBG demodulation system based on wavelength scanning is:

$$f = \frac{pc}{2nmL} \tag{2.3}$$

For determination of wavelength scanning width and step distance, maximum scanning frequency of the demodulation system is limited by sensing distance. For instance, for the 4000 pm scanning width and 16 pm scanning step, at a distance of 2 km, the maximum scanning frequency of the system is 200 Hz. Indeed, the speed of the demodulation system is also limited by FPGA computing power. FPGA starts wavelength calculation to avoid the cumulative overflow of real-time data after the current reflected optical pulse signal is returned. Before the next set of optical pulse signal return, FPGA must calculate the peak wavelength of all uwFBG. For the demodulation system of 200 Hz, the center wavelength demodulation time of the uwFBGs on the whole fiber is less than 5 ms. Considering the frequency of wavelength scanning and the number of uwFBG, the demodulation time of a single uwFBG needs to be calculated accurately. For instance, when the clock period is 8 ns, 264 clock cycles are required for demodulating a single uwFBG. Namely, the time consumption of a single Bragg grating is 2.112 μs. The average time is 2.5 μs, and 2000 uwFBGs can be demodu-

lated within 5 ms. Theoretically, by optimizing the FPGA timing control and fitting algorithm, the system can realize 200 Hz demodulation of 2000 uwFBG with 2 km length and 1 m uwFBG interval and collect dynamic invasion signal on perimeter guardrail.

2.3. Event Recognition Method

The false alarm rate is a crucial parameter of the perimeter security system. It is essential to select an appropriate event recognition methods, specifically involving invasion signal fragmentation, pre-processing, eigenvector extraction, and pattern recognition.

Invasion event is sudden and instantaneous. Invasion signal fragmentation and pre-processing can reduce the system's load and optimize signal quality. When no invasion event occurred, the central wavelength of uwFBG changes little, usually less than 10 pm (see **Figure 2**), and the system did not need to respond. When an invasion event occurs, the optical cable is disturbed. As shown in **Figure 3**, a marked change occurs on the wavelength. The appropriate threshold can be set according to the optical cable arrangement on site. The invasion event can be judged when the wavelength drift exceeds this threshold. The reflective wavelength signal 2 s before and 8 s after the time point was taken as a pre-processing sample. For instance, the uwFBG central wavelength on the optical cable is 1539.310 nm. If the amplitude change exceeds 1539.330 nm, we must fragment the signal from this point. Meanwhile, the wavelet threshold denoising method was used to denoise the vibration signal to obtain a smoother motion, making the convenient processing of convenient data.

The time-domain features of the uwFBG reflected signal are obscure. Still, the frequency distribution is primarily centred in the three frequency bands from 5 to 7 Hz, as illustrated in **Figure 4**. The fast Fourier Transform (FFT) signal below 20 Hz is separated into 20 sub-bands as a pattern recognition eigenvector to decrease the rapid FFT data and increase the accuracy of model classification.

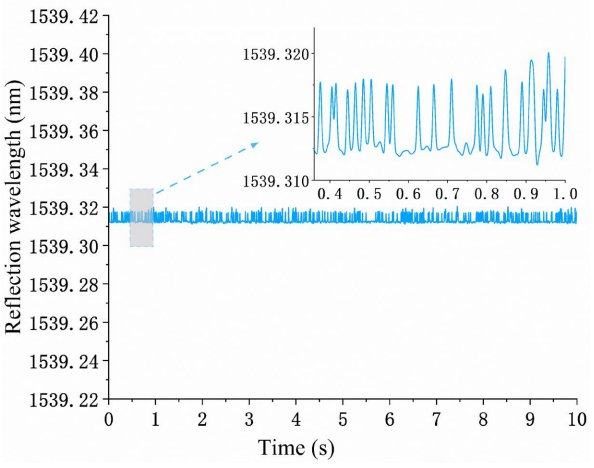

Figure 2. Silent signal collected by the system when no invasion event occurs.

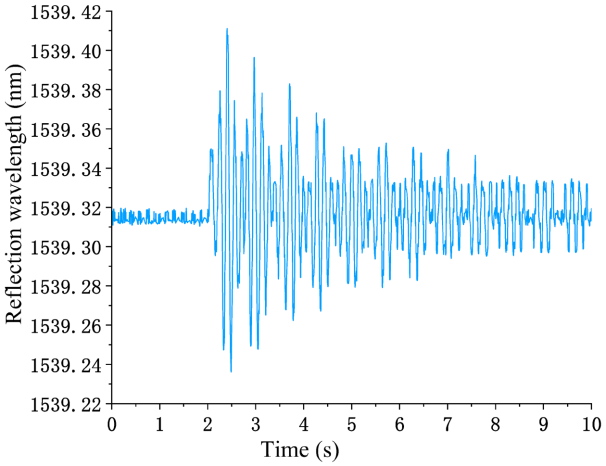

Figure 3. Vibration signal collected by the system when an invasion event occurs.

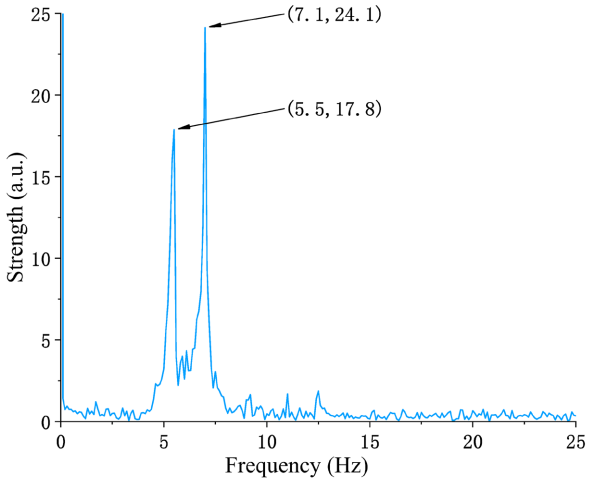

Figure 4. Spectrum diagram of intrusion signal transformed by FFT.

Excluding frequency bands with a high amplitude below 1 Hz, the distribution of the invasion signal is an eigenvector, as depicted in **Figure 5**. The vibrational frequency is primarily concentrated at 5, 6, and 7 Hz. First, fragments of various invasion signals were recovered, followed by a wavelet denoising pretreatment, and then FFT transformation was conducted. Finally, distinct eigenvectors are generated on the frequency domain and entered into the support vector machine (SVM) model for pattern identification, separating the various invasion events.

SVM is a machine learning technique based on the VC dimension theory and the criteria for structural risk minimization [16] [17]. It possesses the benefits of global optimization and full generalizability. The basic idea is to map indivisible data in low latitude to a high dimensional space through nonlinear mapping, in which a hyperplane can be found to separate the two data groups. It ensures the maximum distance between various categories and realizes samples' classification.

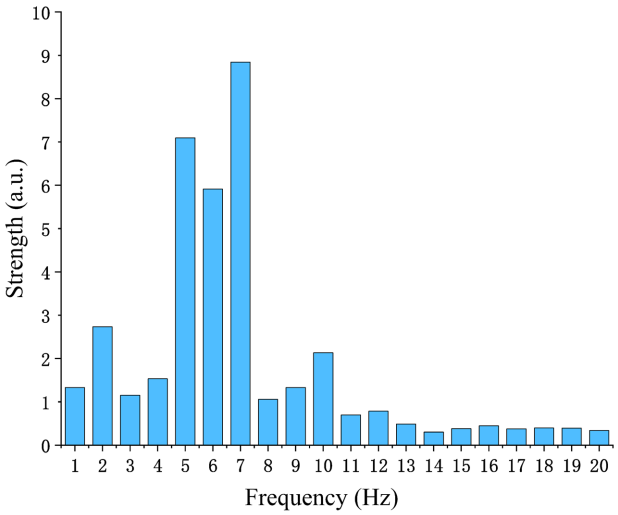

Figure 5. The characteristic vector distribution of intrusion signal spectrum after band division.

given a training sample set $D=\{(x_1,y_1),(x_2,y_2),\cdots,(x_3,y_3)\}$, $y_i\in\{-1,+1\}$, x_i is sample characteristic data, y_i is the data category label. When $y_i=1$, it's the first type of thing; when $y_i=-1$, it is the second kind of thing. If the training sample set is linearly separable, it is assumed that there exists a hyperplane that can separate two types of training samples, with the following equation characterizing it:

$$w^T x+b=0 \tag{2.4}$$

where $w=(w_1,w_2,\cdots,w_n)$ is the parameter of the hyperplane, its dimension is equal to the number of features of the training sample, let's call the hyperplane (w,b), b determines the distance between the hyperplane and the far point. The distance between the hyperplane and the far end is determined by b. Let r represent the distance between each sample inside the sample set and the hyperplane. Then, r is expressed as:

$$r=\frac{\left|w^T x+b\right|}{\|w\|} \tag{2.5}$$

around the separated hyperplane, the training sample point closest to the hyperplane is called the support vector, then the distance between the support vector and the hyperplane is $r=\frac{1}{\|w\|}$. The idea of SVM is to maximize the distance r of the separated hyperplane. solving the following optimization issues determines the hyperplane:

$$\min_{w,b}\|w\| \tag{2.6}$$

$$\text{s.t. } y_i\left(w^T x_i+b\right)\geq 1,\ i=1,2,\cdots,m. \tag{2.7}$$

Herein, SVM was used as the classifier for recognizing invasion events pat-

terns. Sample-based learning can enhance the accuracy of event recognition.

3. Perimeter Security System Performance Tests

To verify the performance of this perimeter security system, select a section from a sensing optical cable that is 2 km long, a diameter of 2.0 mm, and 1000 uwFBG inscribed on it, mounted on a 0.2 km long iron guardrail. The sensing optical cable is tightly coupled with the steel net, and a certain amount of prestressing is applied. The beginning of the thread is connected to the uwFBG demodulation system, and shaking the guardrail simulates two distinct human invasion events. Spraying water to the iron guardrail simulated precipitation weather affecting windy weather by directing a high-powered industrial blower against the iron guardrail and monitoring the vibration signal on the iron guardrail using a perimeter security system to investigate the system's response to four typical events (knock, shaking, precipitation and wind) and its resistance to environmental disruption.

3.1. Determination Accuracy of Invasion Events

To simulate a probable security interference event in the actual world through pounding and shaking, 250 knocks and 250 shakes on the iron guardrail. Each invasion lasts between 3 and 5 s. Adjust the signal fragment wavelength drift threshold to 0.1 nm. When a signal that exceeds the entry is created, an invasion event is determined to have occurred. In digital circuitry, however, occasional burr signals will occur. In the experiment, the signal's amplitude exceeds the wavelength drift threshold and will be misinterpreted as an invasion event by the system. The frequency of these burrs is greater than 20 Hz, but the frequency of the vibrational signal produced by human invasion on a stiff perimeter guardrail is within 20 Hz. The vibrational frequency criterion can filter the burr signal above 20 Hz. **Table 1** displays the determination of accuracy by system invasion event. The combined determination of wavelength threshold and vibrational frequency accuracy increases from 92.4% to 99.2% compared to the single determination approach and 93.2% to 99.6%.

Table 1. Under different decision conditions, the accuracy rate of the system determines intrusion events.

Basis to Judge	Event Type	Times of Test	Determine Number	Determine Accuracy Rate
Wavelength Threshold	Shaking Event	250	231	92.4%
	Knock Event	250	233	93.2%
Wavelength Threshold and Vibrational Frequency	Shaking Event	250	248	99.2%
	Knock Event	250	249	99.6%

3.2. Pattern Recognition Classification

OTDR technology is used to lock the location of the striking and knock event points. As shown in **Figure 6**, at 523 m, the reflection wavelength of the uwFBG at 523 m has a large drift. As a result, the system can position the invasion event. Extract the real-time changes in uwFBG reflective wavelength (see **Figure 7** and **Figure 8**). These two signals are very similar in the time domain. Hard to tell them apart, further processing is required.

An FFT transform was executed on the two forms of invasion event signals, the typical spectrum of knocking and shaking events is depicted in **Figure 9**. The frequency of the vibrating signal generated by a swaying guardrail is predominantly centred between 5 and 7 Hz. The knock limit of vibrational signal frequency is primarily centred at 5 and 9 Hz. **Figure 10** depicts the distribution of invasion signal eigenvector by frequency band. In the frequency region between 5 and 9 Hz, the eigenvectors of two distinct types of invasion signals are strikingly diverse. This is the foundation for classification by SVM. Add a label to

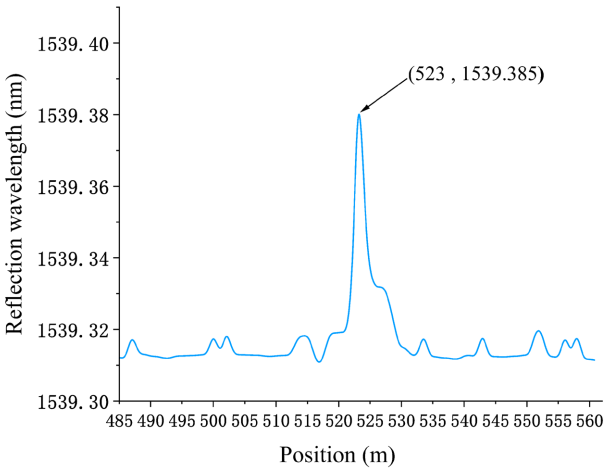

Figure 6. Locate the event location.

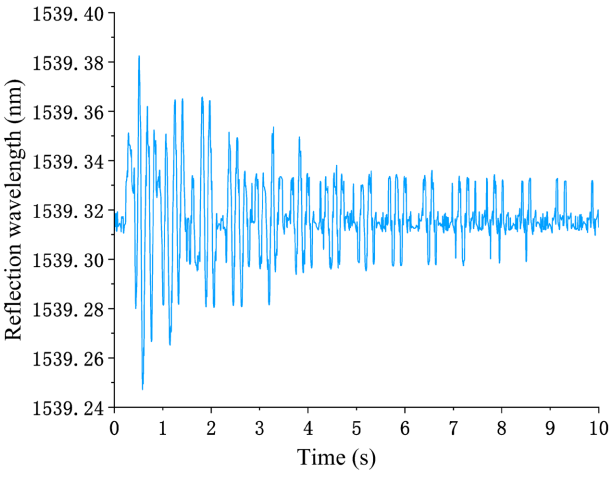

Figure 7. System collected shaking event vibration signal.

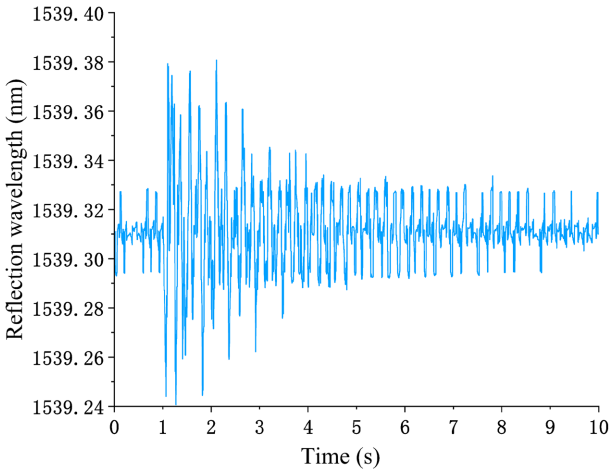

Figure 8. System collected knocking event vibration signal.

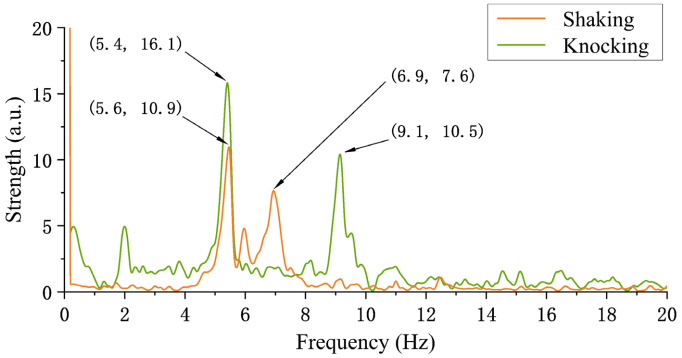

Figure 9. Shaking event and knocking event invasion signal after FFT transform spectrum.

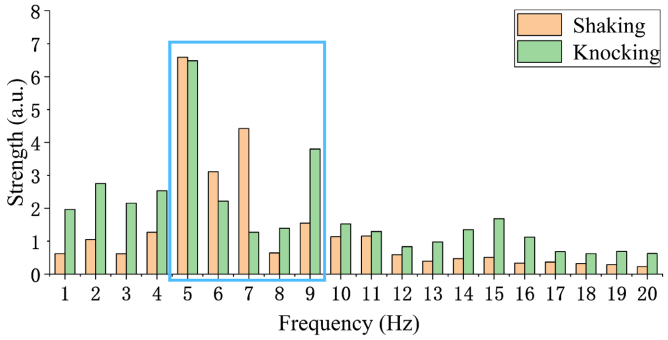

Figure 10. Comparison of the eigenvector distribution of the vibration signal spectrum of two kinds of invasion events division by frequency band.

the two feature data types. Mark knock event as -1, mark shaking event as 1. 400 groups were chosen randomly as the training set for the SVM model, and 100 groups of data were chosen as the testing set. The grid search method was utilized to identify the ideal cg parameters, establish the SVM model, and then classify the testing set using the trained model.

Figure 11 shows the results of classifying 100 groups of invasion event data using SVM pattern recognition, the circle in the illustration represents the actual type of invasion event. The asterisk denotes the result of the SVM model's classification and identification of an invasion event. The coincidence of the circle and asterisk suggests that the model accurately classifies and identifies invasion events. It may be observed that only two groups of test data do not coincide. The system has a suitable identification and classification effect on two types of invasion events, with a 98% accuracy rate.

3.3. Capability of the System to Resist Environmental Interference

Considering the impact of environmental factors like wind and precipitation, collect the vibration signal that simulates the rainfall and wind. As shown in **Figure 12** and **Figure 13**, Bragg grating reflective wavelength variation caused by the two environmental factors does not exceed 0.05 nm, less than the wavelength drift threshold. The value is less than the threshold for a wavelength shift. This is mainly because the uwFBG security system generates the vibration signal through contact invasion and the iron guardrail's robust structure and low

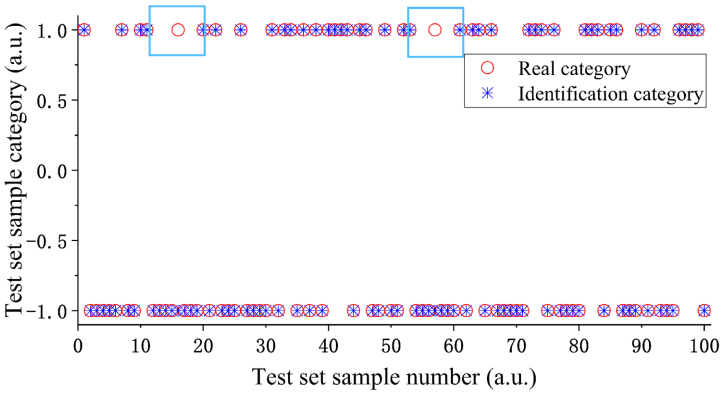

Figure 11. SVM classification and identification effect after training.

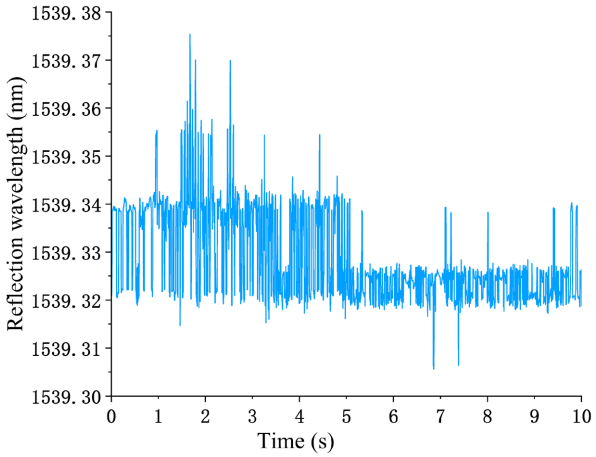

Figure 12. Silent signal collected by the system when no invasion event occurs.

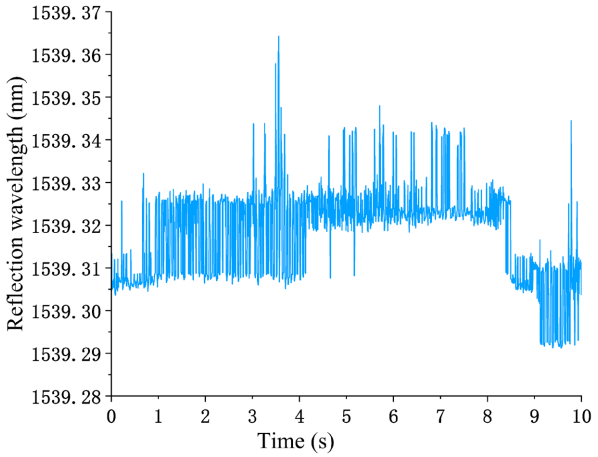

Figure 13. Silent signal collected by the system when no invasion event occurs.

vibrational frequency. Wind and precipitation cannot cause the barrier to shake significantly. Taking into account the influence of two environmental factors as background noise, the accuracy of pattern recognition using SVM still reaches approximately 98%, indicating that invasion event has a negligible effect on the wind and rain environment and that the system has a strong capacity to resist environmental interference.

4. Conclusion

A uwFBG-based, high-speed wavelength demodulation perimeter security system is proposed and established. The system's high-speed demodulation principle and event pattern recognition method are analyzed, and the system performance is tested through experiments. The results demonstrated that the proposed system exhibited high SNR of wavelength demodulation data and could generate real-time responses to an invasion event. The time-domain-frequency-domain joint detection method is adopted to achieve 99.2% and 99.6% alarm accuracy for shaking and knocking, respectively. Shaking and knocking pattern recognition accuracy reached 98% after SVM pattern recognition classification was introduced, indicating good immunity of the system to weather environment and strong resistance to environmental factor interference. This study offers a new scheme for perimeter security.

Conflicts of Interest

The authors declare no conflicts of interest regarding the publication of this paper.

References

[1] Bednarz, B., Popielski, P., Sieńko, R., Howiacki, T. and Bednarski, L. (2021) Distributed Fibre Optic Sensing (DFOS) for Deformation Assessment of Composite Collectors and Pipelines. *Sensors*, **21**, 5904. https://doi.org/10.3390/s21175904

[2] Wijaya, H., Rajeev, P. and Gad, E. (2021) Distributed Optical Fibre Sensor for Infrastructure Monitoring: Field Applications. *Optical Fiber Technology*, **64**, Article ID: 102577. https://doi.org/10.1016/J.YOFTE.2021.102577

[3] Joe, H.E., Yun, H., Jo, S.H., Jun Martin, B.G. and Min, B.K. (2018) A Review on Optical Fiber Sensors for Environmental Monitoring. *International Journal of Precision Engineering and Manufacturing-Green Technology*, **5**, 173-191. https://doi.org/10.1007/s40684-018-0017-6

[4] Yuan, F., Bai, F., Zhu, Y., Cao, Z.B., *et al.* (2020) Research on Automatic Cable Monitoring System Based on Vibration Fibber Optic Sensor Technology. *Journal of Physics: Conference Series*, **1650**, 1-9. https://doi.org/10.1088/1742-6596/1650/2/022010

[5] Wijaya, H., Rajeev, P., Gad, E. and Vivekanamtham, R. (2021) Distributed Optical Fibre Sensor for Condition Monitoring of Mining Conveyor Using Wavelet Transform and Artificial Neural Network. *Structural Control and Health Monitoring*, **28**. https://doi.org/10.1002/STC.2827

[6] Liu, K., Zhang, L.W., Jiang, J.F., *et al.* (2019) Distributed Optical Fiber Sensor pErimeter Security System Based on UAV Video Linkage. *Journal of Optoelectronics·Laser*, **30**, 1244-1251. https://doi.org/10.16136/j.joel.2019.12.0130

[7] Wu, H., Xiao, S., Li, X.Y., Wang, Z.N. and Xu, J.W. (2015) Separation and Determination of the Disturbing Signals in Phase-Sensitive Optical Time Domain Reflectometry (Phi-OTDR). *Journal of Lightwave Technology*, **33**, 3156-3162. https://doi.org/10.1109/JLT.2015.2421953

[8] Zhao, Y., Zhang, S.M. and Wang, B.S. (2020) Research on Performance Characteristics of Fiber-Optic Φ-OTDR Sensor for Travel Safety Incidents Perimeter Security Monitoring System. *Laser Journal*, **41**, 33-37. https://doi.org/10.14016/j.cnki.jgzz.2020.02.033

[9] Yang, N., Zhao, Y. and Chen, J. (2022) Real-Time Φ-OTDR Vibration Event Recognition Based on Image Target Detection. *Sensors*, **22**, 1127. https://doi.org/10.3390/S22031127

[10] Su, Y., Li, S.D., Liu, M.H., Huang, W., Xiao, S. and Xiong, W. (2020) Design and Realization of High Speed Data Acquisition of Φ-OTDR System for Substation Broken Monitoring. *Laser Journal*, **41**, 158-161. https://doi.org/10.14016/j.cnki.jgzz.2020.11.158

[11] Wang, Z., Lu, B., Ye, Q. and Cai, H. (2020) Recent Progress in Distributed Fiber Acoustic Sensing with φ-OTDR. *Sensors*, **20**, 6594. https://doi.org/10.3390/s20226594

[12] Wang, Z.Y., Lu, B., Ye, L., Ying, K. and Sun, Y.G. (2021) Distributed Optical Fiber Acoustic Sensing and Its Application to Seismic Wave Monitoring. *Laser & Optoelectronics Progress*, **58**, 83-94. https://doi.org/10.3788/LOP202158.1306006

[13] Tao, X., Jiang, S. and Song, K. (2020) Low-Cost and Long-Perimeter System Based on Weak Grating Array and Its Alarm Mechanism. *Chinese Journal of Lasers*, **47**, 225-233. https://doi.org/10.3788/CJL202047.0406001

[14] Wang, M., Sun, Z.H., Zhang, L., Wang, B. and Li, Z.Q. (2020) Research of FBG Vibration System Used for Border Security. *Journal of Optoelectronics·Laser*, **31**, 708-712. https://doi.org/10.16136/j.joel.2020.07.0067

[15] Chen, K.K., Li, Y.F., Zhou, C.M. and Fan, D. (2022) Bridge Strain Measurement Based on Weak Fiber Bragg Grating Array. *Laser & Optoelectronics Progress*, **59**, 87-96.

[16] Li, Z.C., Liu, K., Jiang, J.F., Ma, P.F., Li, P.C. and Liu, T.G. (2018) A High-Accuracy Event Discrimination Method in Optical Fiber Perimeter Security System. *Infrared and Laser Engineering*, **47**, 167-172.

[17] Zhang, J.N., Lou, S.Q. and Liang, S. (2017) Study of Pattern Recognition Based on SVM Algorithm for φ-OTDR Distributed Optical Fiber Disturbance Sensing System. *Infrared and Laser Engineering*, **46**, 219-225. https://doi.org/10.3788/IRLA201746.0422003.